JOURNAL OF CATALYSIS 25, 65–80 (1972)

Catalysis by Layer Lattice Silicates. I. The Structure and Thermal Modification of a Synthetic Ammonium Dioctahedral Clay

ALAN C. WRIGHT, WILLIAM T. GRANQUIST, AND JAMES V. KENNEDY

Baroid Division, N L Industries, Inc., P. O. Box 1675, Houston, Texas 77001

Received June 11, 1971; accepted September 28, 1971

The lattice structure of a synthetic ammonium dioctahedral clay (designated SMM) is shown to be similar to muscovite mica. The two differ in that SMM has irregularly interstratified expandable and nonexpandable layers before activation. Thermal activation of SMM causes deamination and a loss of structural hydroxyl, accompanied by a collapse of the interlayer spacing (d_{001}) to 9.4 Å. This dehydroxylation, which probably occurs by pairwise loss of adjacent hydroxyls, is partially reversible leading to high temperature water sorption (P_{H_2O} = 24 Torr, T = 500°C, for example) by activated SMM. During synthesis, F/OH substitutions are possible; the presence of fluoride in hydroxyl sites enhances the water sorption capacity. The appearance of an hydroxyl band at 3470 cm^{-1} in the activated material is attributed to the presence of protons in the tetrahedral vacancies of the octahedral layer. Ammonia and pyridine adsorption experiments show the presence of both Lewis and Brønsted acidity, the relative amounts of each being dependent on the severity of previous outgassing. Total acidity (2.4×10^{19} sites/g) estimated by pyridine adsorption, is small in comparison to that of the zeolitic catalysts (32×10^{19} sites/g). The high activity of SMM is thus believed to be due to decreased diffusion limitations.

Introduction

This paper describes the structure and acidic properties of a synthetic clay-like aluminosilicate which has considerable activity as a catalyst for hydrocarbon reactions. For reasons to be discussed later, the material is designated as SMM, which stands for synthetic mica–montmorillonite. Previously, Granquist and Pollack (*1*) have dealt with the structure and small-scale synthesis of fluoride-free SMM, and Granquist and Kennedy (*2*) have discussed the high temperature (500°C) sorption of water by this substance with particular attention to the roles of lattice fluoride and exchange ions. Later papers will deal extensively with the catalytic properties of SMM, and this writing is designed to present necessary background information.

Unfortunately, due to both the small size of SMM crystallites and the stacking irregularities which occur, single crystal X-ray studies are not possible. Nonetheless, infrared and X-ray diffraction analyses show the relationship of SMM to certain naturally occurring layer silicates and allow reasonable conjecture as to the modifications which take place upon thermal activation.

For coverage of a wide range of information without waste of space or undue confusion to the reader, the paper has been organized on unorthodox lines. It will first relate SMM to the clay minerals in order to orient the reader to the general structural features, deal next with bulk composition, morphology and surface area, and then discuss, for both uncalcined and calcined SMM, structural information obtainable from X-ray and infrared analysis. Because of its importance to catalysis, the heat-activated structure is considered in detail. The

paper closes with a discussion of the adsorptive and acidic properties of the heat-activated mineral, a section based primarily on infrared evidence. Experimental details have been kept to a minimum. Methods are either familiar to everyone in the field, or referenced so that the details can be found elsewhere.

Relationship to Clay Minerals

The infrared spectra of SMM and muscovite mica in the region of their lattice vibrations are compared in Fig. 1. It is apparent that these two materials are quite similar in atomic structure. The small spectral differences which do exist can probably be attributed to the lower lattice aluminum content of SMM, greater (Si,Al) ordering in muscovite, and higher fluoride/hydroxyl substitution in SMM.

The structure of muscovite, from which the structures of dioctahedral clay minerals are inferred, has been well established by single crystal X-ray diffraction studies (*3*). Briefly, the basic layer of muscovite consists, in turn, of three layers, a gibbsitic alumina layer (the octahedral layer) sandwiched between and sharing two-thirds of its oxygens on either side with ($Si_2O_5^-$) sheets (the tetrahedral layers). The remaining oxygens in the octahedral layer belong to the structural hydroxyl groups which project at an angle into each pseudo-hexagonal hole in the tetrahedral layers. Fluoride may substitute in varying degrees for hydroxyl. Because only ⅔ of the cation positions in the octahedral layer are occupied (see Fig. 13A) the term dioctahedral is applied. The entire three layer structure is called a 2:1 layer.

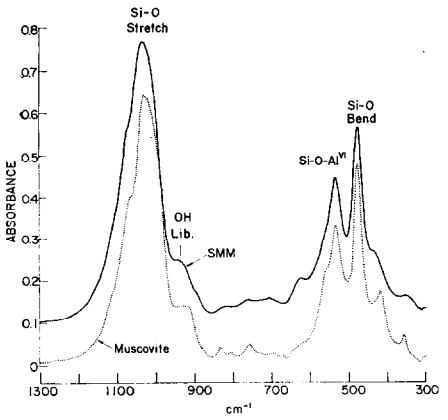

Fig. 1. Comparison of lattice spectra of SMM and muscovite. KBr pellets containing 0.20 mg/cm².

Varying amounts of layer charge are generated by isomorphous substitution in the lattice. In muscovite and SMM the layer charge is caused by partial Al for Si substitution. For both substances, the unit cell formula can be written as

$$[(Al_4)^{octa}(Si_{8-x}Al_x)^{tetra}O_{20}(OH, F)_4]^{x-} \cdot \frac{x}{n} M^{n+},$$

where x is the number of 4-coordinated aluminum cations and hence the net negative charge on the unit cell. M is the charge-balancing cation(s). For muscovite, x is very nearly 2 and $M = K^+$. In the case of SMM, M is predominantly NH_4^+. As discussed in the next section, it is probable that part of the unit cell charge is balanced by a small unknown amount of hydroxy-aluminum species of uncertain charge.

Bulk Composition

Typical uncalcined SMM has a fluoride/silicon ratio of 0.1 and contains 175 meq NH_4^+/100 g (dry basis). If ammonium were the only exchange ion, then knowledge of the bulk composition would allow calculation of the average value of the parameter, x, in the unit cell formula. Such an x value calculated from NH_4^+ content is somewhat smaller than that derived from the silica/alumina ratio, which suggests that not all the aluminum occurs in the lattice. In addition, a weak band at 3440 cm^{-1} in the infrared spectrum can be enhanced by washing SMM with $AlCl_3$ solution. Thus, it seems likely that in addition to NH_4^+, aluminum, or more probably one of its partial hydroxides, also serves as a charge-balancing cation.

Since the average charge on the charge-balancing hydroxyaluminum species is unknown, it is not possible to calculate the average unit cell formula from the bulk composition alone. If, however, M in the unit cell formula is represented by $wNH_4^+ + y[Al(OH)_{3-z}]^{z+}$, mutually com-

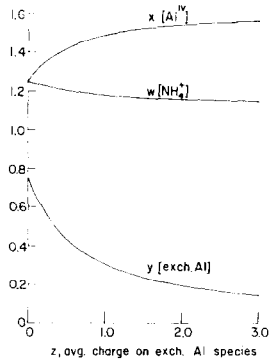

FIG. 2. Mutually compatible w, x, y, and z parameters for unit cell composition

$$[(Al_4)^{oct}\cdot(Si_{8-x}Al_x)^{tetra}\cdot O_{20}(OH, F)_4]\cdot [w\ NH_4^+ + y\ Al(OH)_{3-z}^{z+}].$$

Derived from bulk composition of typical SMM product.

patible w, x, y, and z parameters can be calculated. Figure 2 shows plots of w, x, and y as functions of z, the average hydroxyaluminum charge. For most of the range of z, x lies close to 3/2.

While in theory the correct z value might be found from determination of the relative amount of fourfold-coordinated Al (from apparent AlK_α shift in X-ray spectra, see Ref. *4*) or the loss-on-ignition value, in practice neither figure is a strong function of z and in both cases uncertainties in interpretation arise. The actual per cent Al(IV)[1] observed (about 27% if it is assumed the Al in exchange sites has the same K_α energy as the octahedral Al) indicates a high value for z. The typical ignition loss value (about 9%) at 1000°C after drying at 200°C, however, favors a low value. This loss presumably includes deamination and dehydroxylation of both the silicate and the hydroxyaluminum.

MORPHOLOGY AND SURFACE AREA

Figure 3 is an electron micrograph of SMM before activation and shows the platelike nature of the mineral. The platelets are seen to have average "diameters" on the order of 1000 Å. Individual platelets are made up of stacked parallel 2:1 layers; the exchange ions, which balance the lattice charge, occur between the layers and at the faces of the platelets. The particles which result from spray-drying SMM are spherical aggregations of many platelets.

An estimate of the number of 2:1 layers per platelet may be made from surface area measurements and also from X-ray diffraction data, as will be shown in a later section. At low outgassing temperatures (200°C), the nitrogen BET surface area is typically close to 160 m^2/g. By assuming a platelet diameter of 1000 Å, a density of 2.55 g/cm^3 derived from X-ray unit cell measurements, and inaccessibility of the interlamellar space to the N_2 molecule, the average number of layers per platelet is calculated to be about 5. This value corresponds to an average platelet thickness of 50 Å.

The surface area of SMM is found to be a smooth monotonically decreasing function of the outgassing or pretreatment temperature up to 950°, the temperature at which the structure breaks down and high temperature phases are crystallized. Activation at 650°C causes the surface area to drop from 160 to about 135 m^2/g. Since neither infrared nor X-ray diffraction analyses suggest the development of a new high temperature, low surface area phase, the loss in area can probably be ascribed to increased platelet-to-platelet association.

Of particular importance to catalysis is the large amount of edge area present in SMM. Earlier work (*5*) on clay catalysts and the infrared data to be presented later in this paper suggest that much of the catalytic activity of layer silicates is associated with edge sites.

X-RAY DIFFRACTION

Figures 4 and 5 show X-ray diffractometer patterns (Phillips diffractometer with 1° collimation, Cu tube at 40 kV/30 mA, proportional counter with Ni filter and pulse height analyzer) given by oriented and random samples, respectively, of SMM

[1] The notations (IV) and (VI) designate the coordination state of the aluminum atom, positioning it in either the tetrahedral or octahedral layer, respectively.

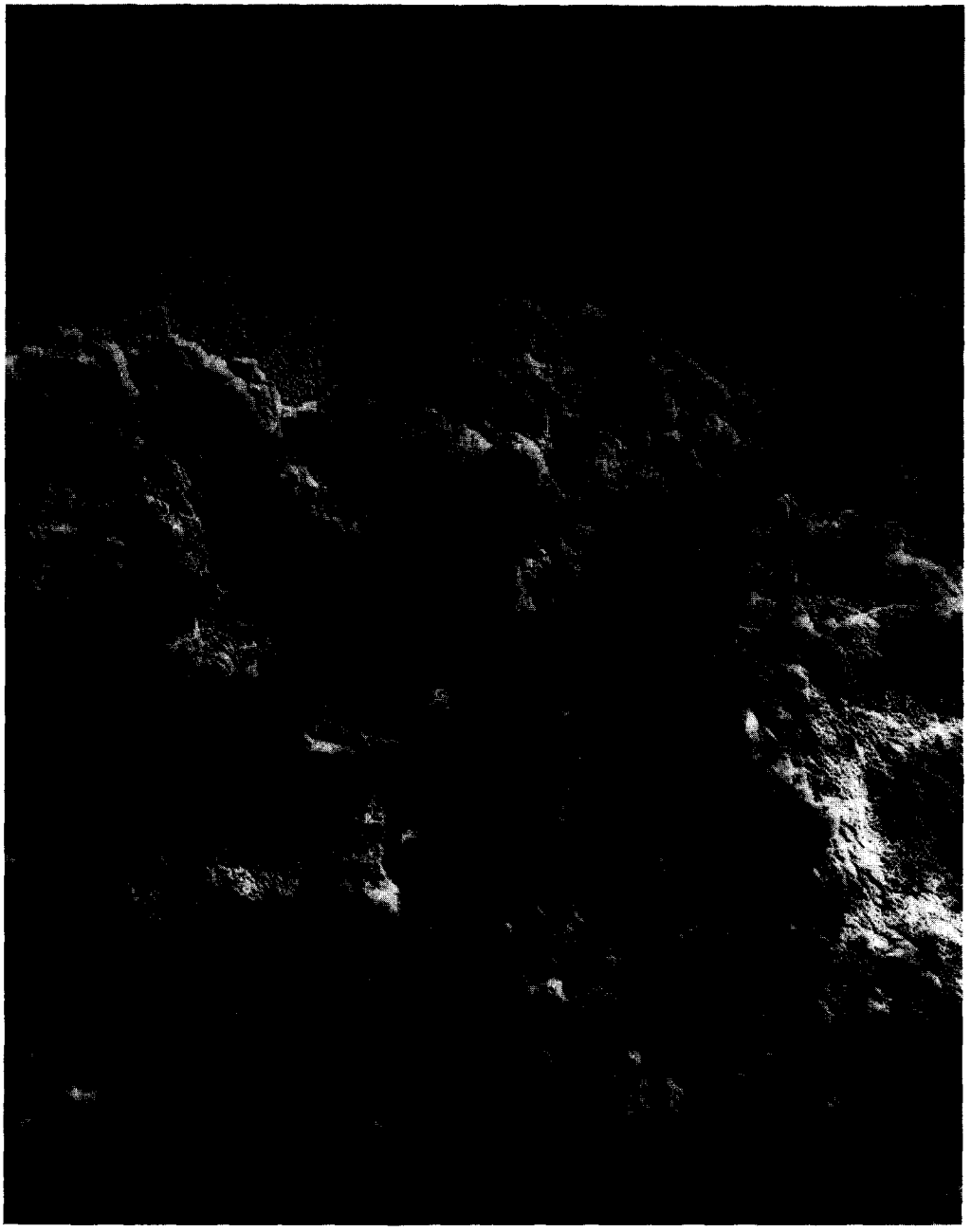

FIG. 3. Electron micrograph of uncalcined SMM.

before and after activation at 650°C for 3 hr in air. The oriented sample was prepared by air drying a (approximately) 2% aqueous slurry on a half-length microscope slide. This procedure caused the platelets to orient parallel to the slide and thus enhanced the basal 00ℓ reflections and suppressed the nonbasal lines. The random patterns were obtained using the standard Phillips backloading holder. Since the spray-dried product was in the form of 20–80 μ spheres, orientation effects are minimized in Fig. 5.

It is apparent from Fig. 4 that uncalcined

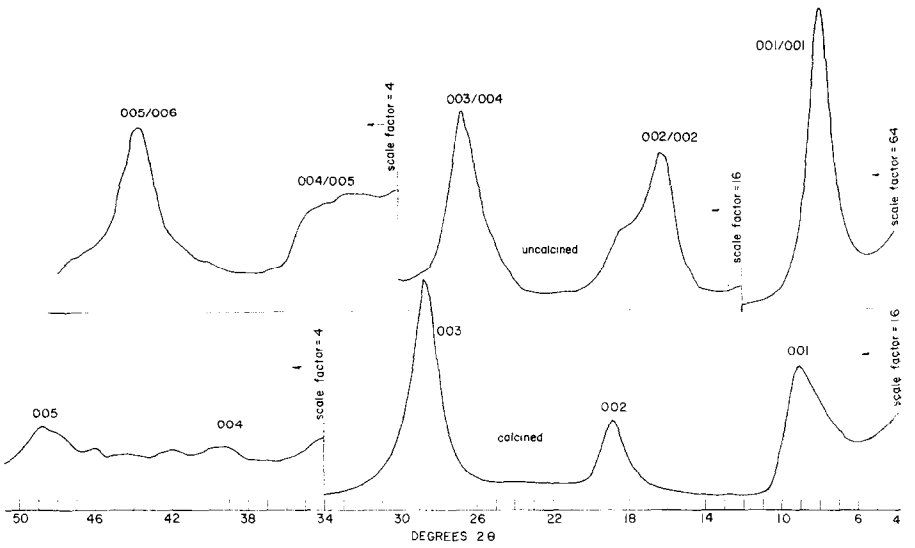

FIG. 4. Oriented X-ray diffraction patterns (Cu K_α) of SMM before and after calcination (650°C for 3 hr in air).

SMM gives a nonintegral 00ℓ sequence with irregularly shaped peaks. This situation, quite commonly encountered in diffraction by clay minerals, is indicative of mixed layering. That is, each platelet contains a nonregular ordering of at least two different basal plane spacings (center-to-center distances between adjacent 2:1 layers).

It is possible to recover information regarding the magnitude of the basal spacings, their relative frequencies, and degree of randomness in order of occurrence by means of a MacEwan transform (*6*). This method is a cosine transform of the oriented diffraction pattern after correction for geometrical, instrumental, and structure factor effects. Figure 6 is the result for an uncalcined sample of SMM. The function $p(R)$ gives the probability of finding a diffracting layer at distance R from the center of any arbitrary layer. If, for example, all of the layers were 10 Å apart, $p(R)$ would have peaks of diminishing intensity (due to the finite height of the platelets) at 0, 10, 20, 30, . . . Å.

In practice the transform must be truncated at some value of $1/d$. This fact coupled with other theoretical and practical limitations, such as imperfectly known

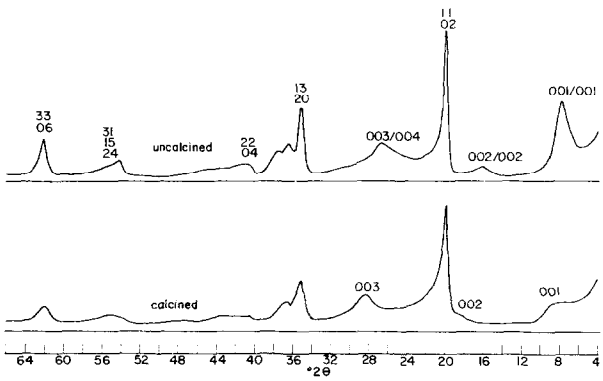

FIG. 5. Random X-ray diffraction patterns (Cu K_α) of SMM before and after calcination (650°C for 3 hr in air). Montmorillonite *hk* indices given.

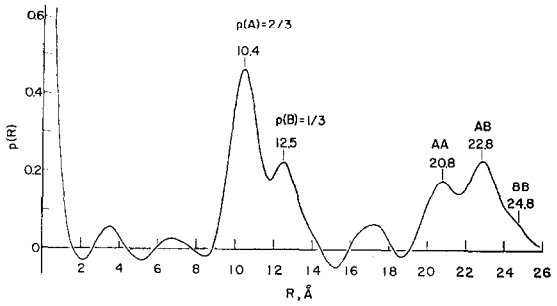

FIG. 6. MacEwan transform for SMM showing probability $p(R)$ of finding 2:1 layer at distance R from center of arbitrary 2:1 layer.

structure factor values and lack of perfect orientation, gives rise to spurious peaks and limited resolution in the $p(R)$ function. Despite these limitations, it seems clear from Fig. 6 that spacings of 10.4 Å (A) and 12.5 Å (B) occur in the proportion 2/1. Analysis of the AA, AB, and BB peak heights indicates that the two spacings occur essentially at random with perhaps a slight tendency for AB ordering.

Scott and Reed (*7*) report a 10.4 Å spacing for ammonium-exchanged muscovite. Quite generally 2:1 clay minerals with one layer of water between the silicate layers have spacings near 12.5 Å (*8*). Thus, the MacEwan transform indicates that SMM has a random interlayering of mica (anhydrous) and montmorillonite-like (hydrated) spacings. Since the mica spacings persist at 100% humidity, these layers (like muscovite) are not readily expandable. The fact that only part of the ammonium in SMM can be easily removed by the usual ion-exchange procedures is also evidence of the micaceous character of the mineral. On the other hand the 12.5 Å spacings exhibit montmorillonite-like behavior in that they swell to 17.3 Å upon addition of ethylene glycol and collapse to about 10.8 Å in dry air.

In dry air, SMM gives an almost integral 00ℓ sequence due to the near equality of the two spacings. Under these circumstances, it is possible to obtain a platelet height estimate (*i.e.*, number of 2:1 layers in a stacking domain) from the diffraction line widths. If a plot of observed half-width vs diffraction order is extrapolated through the origin and a Poisson platelet height distribution assumed, an average thickness of 4.5 layers is obtained. This calculation is in reasonable accord with the platelet size determined from the BET area.

The X-ray pattern given by uncalcined, nonoriented SMM (Fig. 5) is compatible with the concept of mixed layering. If neighboring 2:1 layers were skewed so that no basal (a,b) plane order existed, broad hk bands with low angle band heads would be observed, as is the case with montmorillonite. If these neighboring layers were perfectly ordered with respect to each other then the pattern would have discrete hkl reflections, as in the micas. SMM, in fact, shows evidence of both of these features. While the majority of the nonbasal diffraction maxima resemble those of montmorillonite, the lines near 36° 2θ clearly indicate partial a,b order.

An accurate theoretical calculation of the total diffraction pattern of such a mixed layer clay is for all practical purposes impossible, particularly since micas may have a variety of a,b shifts in their stacking sequences. If it is assumed that the mica layers of SMM are of the 1 M polymorph (*8*) then the unit cell parameters are calculated to be: $a = 5.19$, $b = 8.965$, $c = 10.55$ Å and $\beta = 99°27'$ ($b^2/a^2 = 2.983$).

The diffraction patterns given by heat-activated SMM (the bottom curves in Figs. 4 and 5) clearly show the retention of a high degree of order. Since heat activation is necessary to develop optimum catalytic activity, the irreversible basal spacing collapse to 9.4 Å indicates that only the platelet edges and faces are of catalytic importance. The hk reflections are seen to change very little in position. Thus the dehydroxylation and deamination processes involved in calcination appear to cause only minor alterations in the unit cell structure.

INFRARED ANALYSIS

The laminar nature and drying characteristics of SMM are such that sample preparation for infrared analyses presents no difficulties. Thin selfsupporting films are easily prepared by filtering a dilute slurry through a 0.22 μ Millipore® filter. The film

which forms on the filter is readily removed after air drying and can be cut to a size suitable for infrared examination.

Films prepared in this manner have a high degree of orientation. In some cases this orientation can provide additional information derived from the change in band intensities with angle of beam incidence. On the other hand the relative band intensities of species adsorbed on SMM can be expected to differ from those noted when optically isotropic catalysts such as silica–alumina gels and the synthetic faujasites are used.

The evacuable ir cell has been described in detail elsewhere (*2*). All of the spectra presented in this paper were obtained at room temperature with a Beckman IR 12, purged with dry air, operated in the absorbance mode (linear within 2%) and at 2× the standard slit program. Indene calibration runs showed the wavenumber accuracy to be ±2 cm^{-1}. The wave numbers reported here have not been corrected to vacuum conditions. Depending on the spectral detail being observed, scanning speed varied from 20–80 cm^{-1}/min.

Untreated SMM

The top tracings in Figs. 7 and 9 show the spectrum given by unmodified SMM in the range 1200–4000 cm^{-1} after evacuation to 10^{-5} Torr at 25°C for 2 hr. Similar to other dioctahedral layer aluminosilicates, SMM has a sharp, strong band at 3640 cm^{-1} arising from the O—H stretch of the structural hydroxyls. N—H stretching bands of the ammonium ion occur at 3035 and 3300 cm^{-1}. In agreement with the proposed structure for SMM, Farmer and Russell (*9*) have shown the 3035 cm^{-1} band to occur only in those clay minerals with tetrahedral Al substitution. The strong band at 1432 cm^{-1} and weak band at 1677 cm^{-1} are N—H bending modes. The appearance of the latter is a result of the less-than-cubic symmetry of exchange sites since this band is infrared forbidden for the free ion. The shoulder at 2820 cm^{-1} is probably an overtone of the 1432 cm^{-1} band. A small amount of residual water is evidenced by the absorption at 1650 cm^{-1}.

The small peak at 3440 cm^{-1} is believed to be associated with the previously discussed hydroxyaluminum exchange species. This band is found to persist after all molecular water has been removed and can be enhanced by washing the film with $AlCl_3$ solution and rinsing prior to air drying.

Low Temperature Deuteration

In order to gain further information concerning the mixed layer nature of SMM, a low temperature deuteration study using D_2O vapor (21 Torr) was carried out. Prior to each spectral run, the cell was evacuated for 10 min to remove most of the interlayer D_2O. All evacuations were done at room temperature to minimize dehydroxylation and deamination. Figure 7 shows selected spectra from this experiment. A cross-plot of the integrated absorbances of NH_4^+ vs structural OH and a table of temperature and corresponding contact time for each point are presented in Fig. 8.

It is seen that breaks occur in the cross-plot at A and B. In order to distinguish between deuteration associated with the platelet faces and with the montmorillonite layers, both of which sorb water, a similar experiment was performed using ammonium exchanged rectorite (*10*), a naturally occurring 1:1 regularly interstratified mica/montmorillonite which has proportionately much less platelet face area than SMM. Comparison of the results suggests the following interpretation of Fig. 8. In runs 1–4, the exterior and montmorillonite-associated ammonium ions were deuterated with very little lattice hydroxyl exchange taking place. In runs 5–7, exterior (platelet face) hydroxyls were exchanged with no additional ammonium exchange. Sufficient time and temperature in runs 8–15 allowed slow deuteration of some of the remaining hydrogens.

If the number of 2:1 layers in a platelet has a Poisson distribution centered at 4.5 (from X-ray data), it follows that 30% of the hydroxyls occur in the particle faces; the actual degree of exchange at breakpoint B is 31%. From a knowledge of the ratio of mica to montmorillonite spacings (2/1),

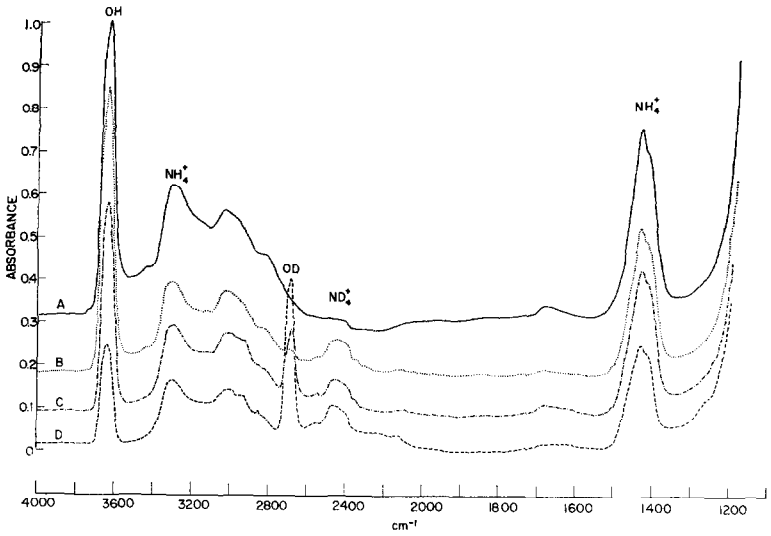

FIG. 7. Selected spectra from low temperature deuteration experiment. Curve A from run 1; B, run 4; C, run 7; D, run 15 (see Table in Fig. 8). Film wt. (fresh) of 1.80 mg/cm².

average unit cell ammonium content (1.16 for this particular experiment), and the fraction of nondeuterated ammonium at breakpoint A (77%), the unit cell ammonium content of the mica layers can be determined. The calculated value of 1.95 agrees quite well with the "ideal" value of 2 for muscovite mica, though this agreement may be fortuitous because of the uncertainty in some of the data.

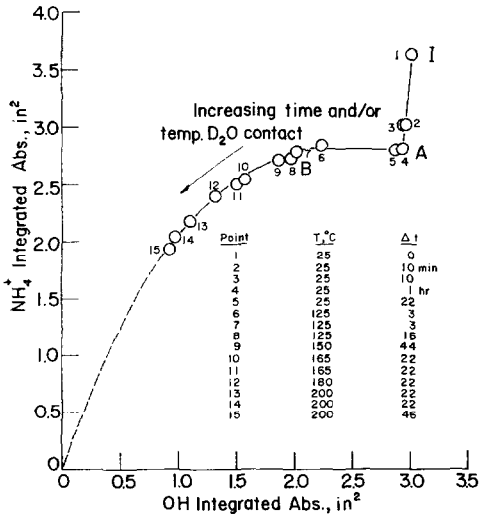

FIG. 8. Cross-plot of integrated intensities at 1432 cm^{-1} NH_4^+ and 3640 cm^{-1} OH bands with table of D_2O (21 Torr) contact times and temperatures.

The spectrum in Fig. 7 taken at breakpoint B shows the hydroxyaluminum band to be almost entirely deuterated, an indication that this species probably does not occur in the mica-like interlamellar spaces. Thus the calculated value of 1.95 NH_4^+ per unit cell should represent the average degree of Al substitution in the tetrahedral layers associated with the mica-like spacings.

Since the average charge z (see Fig. 2) of the hydroxyaluminum species is unknown, it is not possible to calculate the average degree of substitution in the nonmicaceous tetrahedral layers. By assuming various values of z, however, a range of substitution values may be established. For this particular case, the Al for Si substitutional parameter in these layers is found to be 0.59, 0.99, 1.09 and 1.15 for z equal to 0, 1, 2 and 3, respectively. (Note that the values of x plotted in Fig. 2 refer to the bulk composition composed of both kinds of layers.) It seems clear that the difference between the mica and montmorillonite-like layers is at least in part due to a real compositional variation in the lattice.

Dehydroxylation and Deamination

Of greater interest to catalysis is the structure of SMM after thermal activation. The overall reactions which occur are loss

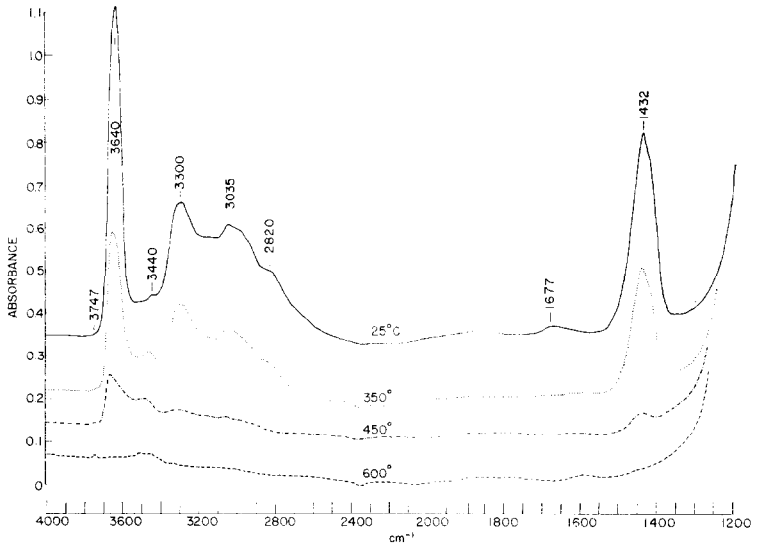

FIG. 9. Selected spectra from vacuum activation experiment. Film wt. (fresh) of 1.77 mg/cm².

of ammonia, with accompanying release of protons to the lattice, and dehydroxylation. These reactions, which occur simultaneously to a large extent, are easily followed by infrared analysis.

Figure 9 shows selected spectra of the same sample of SMM, uncalcined at the start of the experiment, after heating for 2 hr at 50°C increments under vacuum conditions ($<10^{-5}$ Torr, typically). A plot of the integrated absorbances of the 3640 cm^{-1} hydroxyl and 1432 cm^{-1} ammonium bands vs temperature is given in Fig. 10.

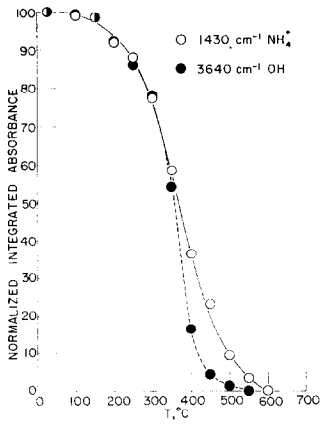

FIG. 10. Integrated NH_4^+ and OH peak intensities vs vacuum activation temperature. Peak areas normalized to 100 for fresh SMM.

It is apparent that in the early stages of activation the ammonia loss closely parallels hydroxyl loss. Final deamination, however, somewhat precedes final dehydroxylation.

During the deamination process the hydroxyl band shifts from 3640 to 3670 cm^{-1}. This shift probably results from the change in exchange cation ($NH_4^+ \rightarrow H^+$) since it has been observed (*11*) that the hydroxyl frequency of clay minerals is somewhat dependent on the nature of the charge-balancing ions. A band at 3470 cm^{-1} also develops during deamination. The growth of this band is not easily followed because of the simultaneous decrease in the 3440 cm^{-1} hydroxy-aluminum band. Though it is not obvious from Fig. 9, subtraction of the residual ammonium absorption in the region 2200–3500 cm^{-1} shows that a broad band covering this region appears concurrently with the 3470 cm^{-1} band. Since both of these features appear more clearly in the spectra dealing with the rehydration characteristics of SMM, they will be discussed in more detail later.

The spectra in Fig. 9 also show a small, sharp peak at 3747 cm^{-1}. This band is believed to arise from edge silanol groups since it is perturbed by adsorbed species such as water, ammonia, and pyridine, and can be readily deuterated by D_2O vapor.

Similar experiments with fluoride-free

SMM differ in two respects. First, the absence of fluoride lowers by approximately 100°C the final loss of 3670 cm^{-1} hydroxyl. Second, the 3470 cm^{-1} band persists to higher temperatures when fluoride is absent.

Rehydration of Activated SMM

One of the unusual properties of calcined SMM is its ability to sorb appreciable water at elevated temperatures. Granquist and Kennedy (*2*) demonstrated that SMM sorbs about 1% water at 490°C and 24 Torr H_2O vapor pressure, and that lattice fluoride appears to be responsible for much of this uptake.

Infrared studies show that such sorption is accompanied by partial regeneration of structural hydroxyl. Rehydroxylation is an activated process which proceeds very slowly at room temperature, but approaches apparent equilibrium within several hours at 200°C. The word "apparent" is used because at P_{H_2O} = 24 Torr the reaction virtually ceases after recovery of only about 35% of the original hydroxyl band intensity. This amount roughly corresponds to the percentage of hydroxyl which occurs in the 2:1 layers making up the faces of the platelets after allowance for the decrease in surface area upon activation. To rehydroxylate the interior 2:1 layers of a given stacking domain, high temperature and higher H_2O vapor pressures would be required, since a dehydroxylation/rehydroxylation process giving net H_2O transport between the layers probably is involved.

The top tracing in Fig. 11 is the spectrum of the clay film used in Fig. 9 after rehydration at P_{H_2O} = 24 Torr and 400°C for 16 hr. The lower spectra show the effect of heating at 100°C increments for 2 hr under vacuum. It is seen that in addition to the lattice hydroxyl band, the 3470 cm^{-1} band and the apparently associated 2200–3500 cm^{-1} underlying absorption are also regenerated by H_2O addition. These latter two features are observed to exhibit greater temperature stability than the 3670 cm^{-1} band. The 3470 cm^{-1} band appears to become a doublet having components at 3450 and 3510 cm^{-1} as dehydroxylation proceeds. Because of the breadth of the bands it is possible that this doublet is actually present in the upper spectra but masked by a less stable 3470 cm^{-1} component.

The 3670 and 3470 cm^{-1} bands and the underlying absorption are readily deuterated by D_2O vapor. The effect of 1.5-hr contact time at 110°C is shown in Fig. 12. Comparison of the O—D and O—H bands, with compensation for the decreased intensity of O—D vs O—H, leads to the conclusion that all three features are about 60% exchanged. Further, the H,D exchange seems to proceed at the same rate for these three features, an observation suggestive of a high degree of proton mobility.

Discussion of Activated Structure

The structure of dehydroxylated dioctahedral clay minerals is a subject of con-

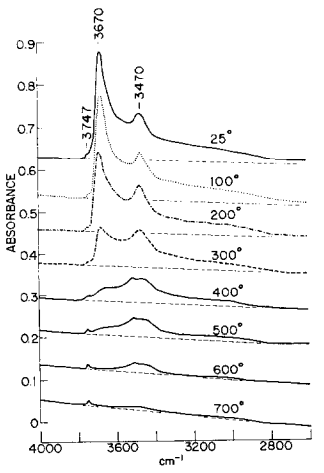

Fig. 11. OH stretch region spectra showing thermal behavior of partially rehydroxylated SMM. Film wt. (fresh) of 1.77 mg/cm².

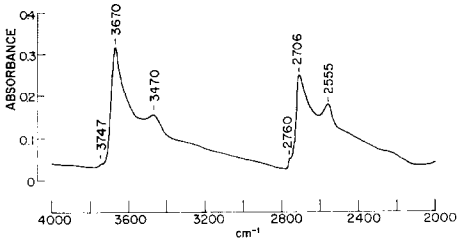

Fig. 12. Spectra showing OD–OH exchange of partially rehydroxylated (H_2O) SMM (see text). Film wt. (fresh) of 4.76 mg/cm².

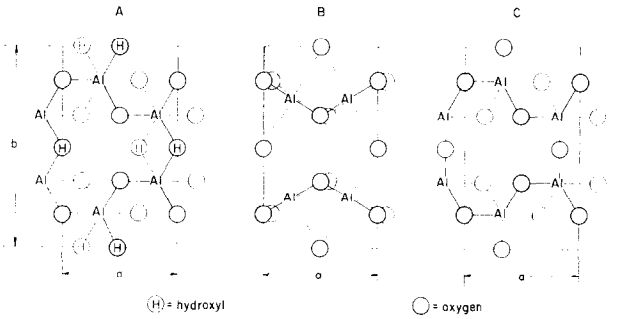

FIG. 13. Octahedral layer of dioctahedral clay minerals. A: before dehydroxylation; B: after dehydroxylation (Bradley and Grim); C: after dehydroxylation (Wright, Granquist and Kennedy).

troversy (*12*). The high degree of variability possible for these materials, in terms of lattice substitution and charge-balancing ions, is no doubt responsible for much of the confusion. For SMM the most pertinent studies are those involving muscovite. The ideas set forth here, while based on such studies and encompassing our results on SMM, should be considered as working hypotheses.

Despite the exfoliation which usually occurs when muscovite is rapidly dehydroxylated, a crystalline structure remains. From a high temperature, high pressure infrared study, Vedder and Wilkins (*13*) concluded that the reaction is probably reversible. Eberhart (*14*) has shown by one-dimensional Fourier synthesis that the net result of dehydroxylation is a loss of four oxygens from their normal positions (± 1.1 Å) in the octahedral layer and a gain of two oxygens at the center of the 2:1 layer (0 Å). To explain his data he favors the Bradley and Grim (*15*) octahedral layer arrangement shown in Fig. 13B.

An alternate arrangement, which also accommodates Eberhart's one-dimensional synthesis and which easily explains various observations on SMM, is shown in Fig. 13C. This alteration occurs with minimum disruption of the unit cell, in agreement with the fact that the strong features of the lattice infrared spectra of both SMM and muscovite change very little upon dehydroxylation. In addition, the ease with which SMM partially rehydroxylates under moderate conditions is more readily understood since a concerted movement of many atoms is not required. The overall equilibrium process can be represented schematically as shown below.

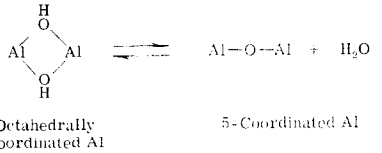

A complicating factor is the presence of fluoride proxying for hydroxyl (about 0.65 F^-/unit cell). Dehydroxylation of an (OH,F) pair should take place with greater difficulty since the loss of either a proton or a hydroxyl from such a pair would result in a charged species. This situation is in agreement with the observation noted earlier that fluoride-free SMM undergoes final dehydroxylation more easily than the usual product. Conversely, once dehydroxylated, fluoride-containing SMM should more readily take up water at high temperatures in accord with the observations of Granquist and Kennedy (*2*).

It is probable that the protons resulting from the deamination process do not remain in the interlamellar space, but rather enter sites in the aluminosilicate lattice. Such protons, about 1.15 H^+/unit cell, can be considered "excess" in a structural sense, since they were initially exterior to the 2:1 layer structure. Use of the term "excess protons" does not imply any charge imbalance; in fact, these protons are charge-balancing ions.

Part of the excess protons are probably lost by the reaction

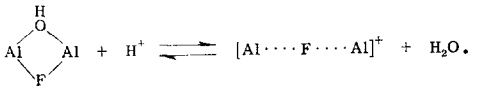

The resulting species assumes the charge-balancing role of the proton lost in the reaction.

The fate of the remaining protons remains a puzzle. That these protons are eventually lost is shown by the complete absence of OH bands in the infrared (other than the small 3747 cm^{-1} band) after 24 hr of evacuation at 650°C. Perhaps a mechanism similar to that proposed by Uytterhoeven, Christner, and Hall (*16*) for ammonium faujasites is also operative here; i.e.,

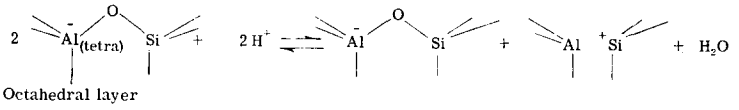

This process generates Lewis sites in the tetrahedral layers. Studies of pyridine sorption, to be discussed later, do show the development of another type of Lewis site under extremely anhydrous conditions, but the density of such sites seems too small to correspond to removal of remaining protons by the above mechanism.

Steam purging of SMM under severe conditions (760°C, 15 psi flowing steam) causes a gradual loss of fluoride. A possible explanation for this phenomenon is the small but finite probability for HF loss from the (OH,F) pairs; i.e.,

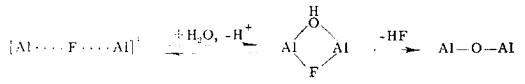

Analytical data suggest that any liberated HF immediately reacts with the silicate lattice to form SiF_4 which in the presence of steam is converted to H_2SiF_6.

Russell and White (*17*) report that the development of a 3470 cm^{-1} band by thermal treatment is characteristic of ammonium or hydrogen dioctahedral clays containing 4-fold coordinated aluminum. In agreement with their findings, sodium exchanged SMM shows neither this band nor the underlying 3500–2200 cm^{-1} absorption during dehydroxylation or rehydration. It seems certain that these two features are in some manner associated with the excess protons in the deaminated mineral. Because the presence of fluoride allows loss of some of the protons by the mechanism discussed earlier, the 3470 cm^{-1} band occurs more strongly in fluoride-free SMM at high temperatures. Though comparable levels of hydration are difficult to achieve, comparison of fluoride-containing to fluoride-free SMM also appears to show that lattice fluoride considerably enhances the broad underlying band.

Russell and White (*17*) believe the 3470 cm^{-1} band to be due to proton perturbed lattice hydroxyl groups. The presence of an electron withdrawing excess proton near the oxygen of an hydroxyl group would be expected to weaken the O—H bond and thus lower its stretching frequency. As convincing evidence for their assignment they showed that addition of ammonia causes disappearance of the 3470 cm^{-1} band with regeneration of ammonium ion and unperturbed lattice hydroxyl.

Experiments involving addition of both ammonia and pyridine vapor demonstrate the same effect for activated SMM. Figure 14 shows the spectrum of the hydroxyl region of activated SMM before and after pyridine addition. The curves are displaced horizontally to aid comparison of peak heights. The addition of pyridine causes generation of pyridinium. Very similar spectra result when ammonia is added. These effects will be discussed in a later section of this paper.

Additional evidence for the assignment of Russell and White is provided by orientation studies. The 3670 and 3470 cm^{-1} bands are found to change in intensity in the same manner (±2%) as the angle of incidence of the infrared beam is varied (up to about 60° from normal). Thus the hydroxyl groups giving rise to these bands must have

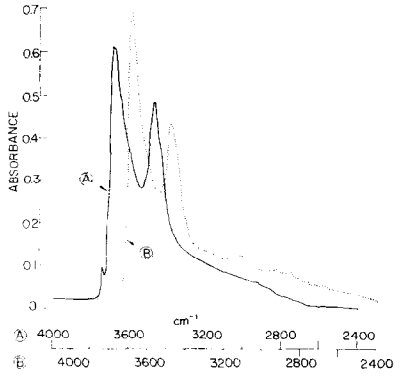

FIG. 14. OH spectra of partially rehydroxylated SMM before (A) and after (B) pyridine adsorption (room temp. vapor pressure for 30 min at 150°C followed by 1 hr evacuation at 150°C). Film wt. (fresh) of 8.85 mg/cm².

very nearly the same average angle of inclination from the basal plane.

Any structure for the proton perturbed hydroxyls must be largely speculative. Russell and White (*17*) schematically show the proton associated with both a lone structural hydroxyl oxygen and the octahedral-layer oxygen belonging to 4-fold coordinated aluminum. It is difficult to see how a lone hydroxyl can exist in the absence of fluoride since reversible dehydroxylation would seem to require the pairwise loss of adjacent hydroxyls. Yet it is an experimental fact that the 3470 cm^{-1} band can exist in the absence of the 3670 cm^{-1} band. Hence a pairwise perturbation of the hydroxyls appears to be more likely.

One hypothesis which accounts for many of the experimental observations is that the protons drop into the empty tetrahedra adjacent to the (OH,OH) or (OH,F) pairs in the octahedral layer (Fig. 13A). A side view of the proposed structure is shown below. The actual bonding of the tetrahedral proton would probably involve resonant associations with all four oxygens.

Such tetrahedral protons would be expected to generate a doublet (previously described in the section on rehydration) because their associated hydroxyls are no longer symmetrically equivalent. Even if fluoride were present a doublet might result if the two tetrahedra have about equal site energies. Actually the situation may be considerably more complex since the degree of perturbation is likely to be a function of the number and disposition of the aluminum tetrahedra sharing oxygens with the site tetrahedra. In any case, a multiplet structure in the perturbed band would be expected.

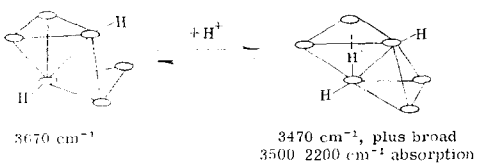

3670 cm^{-1} 3470 cm^{-1}, plus broad 3500–2200 cm^{-1} absorption

The underlying 3500–2200 cm^{-1} absorption can be attributed to the translational motions of the tetrahedral protons. It is reasonable to expect the presence of fluoride to enhance this band. Another possible assignment for the broad absorption is the O—H stretch of hydronium ions. It seems unlikely, however, that this ion could fit in the small interlamellar space left after activation. If hydronium were a surface species, deuteration should be rapid and total, contrary to observation. In addition, this band is observed to form during the initial deamination process. It is doubtful that hydronium would have greater stability than ammonium even with allowance for steric effects.

Several objections to this proposal can be raised. The quantitative measurements of Russell and White (*17*) indicate the regeneration of only one, rather than two, unperturbed hydroxyls for each ammonium ion formed upon ammonia addition. Due to the quartz optics used in their study, they were unable to observe the 1430 cm^{-1} ammonium band and instead used the N—H stretch for their measurements. Possibly the presence of adsorbed ammonia caused an overestimate for the amount of regenerated ammonium. In order to help resolve this issue, similar work on fluoride-free SMM is planned.

In order to account for the high thermal stability of the proton-perturbed hydroxyl band, the tetrahedral site energy for the proton must be very favorable. If this is so then why is the band not observed in natural clay minerals? Hydrogen is itself the

least energetically favored exchange ion and other ions such as sodium, potassium, or calcium are highly preferred. It is only in comparison to other possible *proton* sites that the tetrahedral site is favored.

The greater thermal stability of metal cation clays compared to ammonium or hydrogen clays suggests that the dehydroxylation is proton catalyzed. That this dehydroxylation process must be highly specific

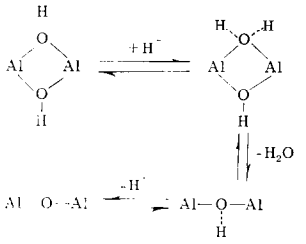

from a steric point of view is one further implication of this tetrahedral proton hypothesis. If this were not true then one might envision the tetrahedral protons simply combining from the interior with hydroxyls to give water molecules which leave via the hexagonal cavities in the tetrahedral layer. However, if it is assumed that the proton attack on an hydroxyl must come from outside the octahedral layer, the special stability of the perturbed hydroxyls is understandable since a tetrahedral proton would repel the approach of the attacking proton.

Adsorptive and Acidic Properties of Activated SMM

Water

Adsorbed molecular water is held with moderate tenacity by activated SMM. Evacuation at temperatures in excess of 150°C is necessary to completely eliminate water as evidenced by its bending mode band at 1650 cm^{-1}. A reduction in intensity of the 3747 cm^{-1} peak when adsorbed water is present indicates some interaction of the edge silanol groups. No evidence is seen for the formation of hydronium ion, though the broad spectral features of this species make detection difficult.

Ammonia

Addition of ammonia (100 Torr for ½ hr at 170°C followed by evacuation for ½ hr at 150°C) to completely dehydrated SMM results in the formation of small amounts of ammonium ion plus Lewis-bound ammonia. The ammonium is apparently formed by reaction with the edge silanol groups since the 3747 cm^{-1} band loses about ⅓ of its intensity. Weak bands occurring at 1620, 1680, 3280 and 3340 cm^{-1} are believed to arise from ammonia at Lewis sites. From the overall lack of intensity in the bands indicative of sorbed species, it is estimated that no more than 5 meq ammonia/100 g is present on the clay under these conditions.

As previously discussed with reference to the 3470 cm^{-1} hydroxyl band, ammonia reacts with partially hydroxylated SMM to form larger amounts of ammonium as well as the above mentioned Lewis-bound species. From measurements of the 1432 cm^{-1} band it was found that a film which has been exposed to NH_3 (1 atm at 150°C for 3 hr followed by evacuation at 70°C for 16 hr) contained 11 meq ammonium/100 g.

Pyridine

The use of pyridine to characterize acidic sites has become almost routine for several reasons (see, for example, Ward (*18*)). First, pyridine is a weak Brønsted base and thus should interact only with the stronger, more catalytically interesting protonic sites. Second, the bands of the adsorbed species are sharp allowing easy distinction between pyridinium ion and Lewis-bound pyridine. In addition, the frequency of the line considered most diagnostic of Lewis-bound pyridine (near 1450 cm^{-1}) gives an indication of the site strength.

Spectrum *b* in Fig. 15 was taken after addition of excess pyridine (30 min at 150°C followed by 2.5-hr evacuation at 200°C) to a film of dehydroxylated SMM. The small peak at 1547 cm^{-1}, characteristic of pyridinium, is formed at the expense of the 3747 cm^{-1} edge silanol band. At least two species of Lewis-bound pyridine are evidenced by the lines at 1463 and 1456

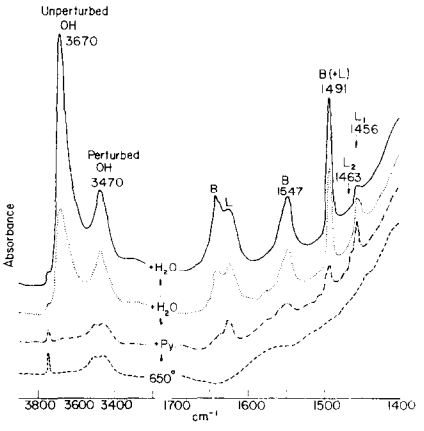

FIG. 15. Pyridine adsorption on dehydroxylated SMM followed by incremental addition of H_2O (see text). 4× scale expansion used in 1400–1700 cm^{-1} region.

cm^{-1}. The former is found to be more tightly held if evacuation at elevated temperature is carried out at this point. Spectra *c* and *d* show the effect of successive additions of about 15 mmol H_2O/100 g clay (no evacuation; 14 hr at 200°C equilibrium). Though most of the water is observed to rehydroxylate the clay, a conversion of Lewis- to Brønsted-bound pyridine is seen. The 1463 cm^{-1} site is also destroyed by water addition.

When pyridine is added to partially hydroxylated SMM the proportion of Lewis- to Brønsted-bound species is found to be a strong function of the residual water content of the film. If previous evacuation is carried out at room temperature only, almost all of the pyridine is sorbed as pyridinium ion. Previous evacuation at 200°C results in approximately equal amounts of the two species. Quantitative measurements suggest a reversible one-to-one interconversion of sites.

The integrated absorption coefficients of Hughes and White (*19*) were used to estimate the absolute numbers of pyridine sites on activated, partially hydroxylated SMM (evacuated at 150°C for 1 hr). (In typical catalytic use, SMM will have appreciable structural hydroxyl.) Changing the angle of infrared beam incidence did not dramatically change the 1547 and 1456 cm^{-1} peak intensities so orientation effects probably were not large. Values of 2.5 meq Brønsted- and 1.5 meq Lewis-bound pyridine per 100 g clay were calculated, giving a total acidity of 4 meq/100 g. Considering the uncertainties involved, this latter figure corresponds well with the result, 3 meq/100 g, of gravimetric measurements using a quartz spring balance.

Discussion of Acidity

If the structural discussion of activated SMM is correct, evidence that both the particle edges and faces contribute to the acidity of SMM is provided by the pyridine sorption experiments. That the face regions are involved is shown by the change in the 3470 cm^{-1} band when pyridine is sorbed. The presence of a tetrahedral proton would be expected to greatly enhance the acidity of the associated structural hydroxyls. Thus the following equilibria may hold:

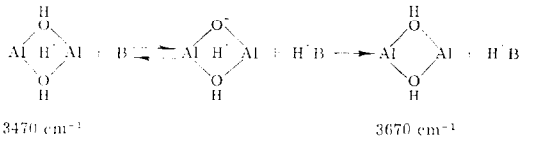

The Lewis acidity of partially hydroxylated SMM can most reasonably be attributed to trigonal aluminum at the edge of the tetrahedral layers. If all of the edge tetrahedral aluminums were involved, about 20 meq/100 g of acidity would be anticipated. That the actual amount of Lewis acidity is less is not surprising since only a fraction of these aluminums would have a trigonal configuration. The conversion of these sites from Lewis to Brønsted by addition of water probably occurs as shown below.

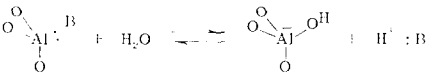

In view of the high catalytic activity of SMM, the density of acidic sites as measured by pyridine, 2.4×10^{19}/g, seems surprisingly low compared to the site density of 32×10^{19}/g reported for faujasites (*19*). (This difference is greatly reduced, however, if site density is expressed on the basis of unit area: SMM, 1.7×10^{17} sites/m^2; syn-

thetic faujasite, 5×10^{17} sites/m^2.) The probable explanation for this apparent discrepancy lies in the respective geometries of the catalysts. Because of the plate-like, poreless structure of SMM, the measured acidity is likely to be representative of the useful acidity. In contrast, due to diffusion limitations, only a small fraction of the measured acidity of zeolites is actually useful under dynamic conditions (*20*).

Acknowledgments

The authors wish to express their appreciation to the Baroid Division, NL INDUSTRIES, INC. for supporting this work and granting permission for publication.

Thanks are also due to Dr. D. A. Hickson of the Chevron Research Company, Richmond, CA, for supplying the electron micrograph, and to Dr. James L. McAtee of Baylor University for many useful discussions.

References

1. Granquist, W. T., and Pollack, S. S., *Amer. Mineral.* **52**, 212 (1967).
2. Granquist, W. T., and Kennedy, J. V., "Clays and Clay Minerals, Proceedings of the 15th Conference," p. 103. Pergamon Press, New York, 1967.
3. Grim, R. E., "Clay Mineralogy," 2nd ed. McGraw-Hill, New York, 1968.
4. White, E. W., McKinstry, H. A., and Bates, T. F., *in* "Advances in X-Ray Analysis" (W. M. Mueller, Ed.), Vol. 21, p. 239. Plenum Press, New York, 1960.
5. Oblad, A. G., Milliken, T. H., Jr., and Mills, G. A., "Advances in Catalysis," Vol. 3, p. 199. Academic Press, New York, 1951.
6. MacEwan, D. M. C., *Koll. Zeit.* **149** (2), 96 (1956).
7. Scott, A. D., and Reed, M. G., "Clays and Clay Minerals, Proceedings of the 13th Conference," p. 247. Pergamon Press, New York, 1966.
8. Brown, G. (ed.), "The X-Ray Identification and Crystal Structures of Clay Minerals," Chap. 5. Mineralogical Society, London, 1961.
9. Farmer, V. C., and Russell, J. D., "Clays and Clay Minerals, Proceedings of the 15th Conference," p. 121. Pergamon Press, New York, 1967.
10. Brown, G., and Weir, A. H., "International Clay Conference, Proceedings of the 1963 Conference," Vol. 2, p. 87, Pergamon Press, New York, 1965.
11. Chaussidon, J., *Clays Clay Minerals* **18** (3), 139 (1970).
12. Grim, R. E., "Clay Mineralogy," 2nd ed. p. 313. McGraw-Hill, New York, 1968.
13. Vedder, W., and Wilkens, R. W. T., *Amer. Mineral.* **54**, 482 (1969).
14. Eberhart, J. P., *Bull. Soc. Fr. Mineral. Cryst.* **86**, 213 (1963).
15. Bradley, W. F., and Grim, R. E., *Amer. Mineral.* **36**, 182 (1951).
16. Uytterhoeven, J. B., Christner, L. G., and Hall, W. K., *J. Phys. Chem.* **69**, 2117 (1965).
17. Russell, J. D., and White, J. L., "Clays and Clay Minerals, Proceedings of the 14th Conference," p. 181. Pergamon Press, New York, 1966.
18. Ward, J. W., *J. Catal.* **9**, 225 (1967).
19. Hughes, T. R., and White, H. M., *J. Phys. Chem.* **71**(7), 2192 (1967).
20. Thomas, C. C., and Barmby D. S., *J. Catal.* **12**, 341 (1968).